

CHROM. 6004

## RESOLUTION IN NON-LINEAR CHROMATOGRAPHY

T. S. BUYS\* AND K. DE CLERK

*Chromatographic Research Unit of the South African Council for Scientific and Industrial Research, Department of Physical and Theoretical Chemistry, University of Pretoria (South Africa)*

(Received February 7th, 1972)

## SUMMARY

The available expressions for the statistical moments in non-linear chromatography are used to formulate an approximate expression for the resolution function in terms of column parameters.

## INTRODUCTION

Chromatographic peaks resulting from a non-linear distribution isotherm are in general, asymmetrical. It has been shown that, if these peaks are fitted by bi-Gaussian distribution functions<sup>1</sup>, the resolution function (see Fig. 1)

$$R_{msa} = \frac{\zeta_2 - \zeta_1}{2(\sigma_{12} + \sigma_{21})} \quad (1)$$

may be related to the efficiency of the separation<sup>2</sup>. (The efficiency criterion is taken as the impurity ratio of the smaller peak<sup>2</sup>.) The aim of the present study is to solve the remaining problem, namely, to rewrite the resolution function in terms of column parameters. For this purpose the function  $R_{nl}$  defined by

$$R_{nl} = \frac{\langle \zeta \rangle_2 - \langle \zeta \rangle_1}{2(\sigma_1 + \sigma_2)} \quad (2)$$

was used.  $R_{nl}$  approximates  $R_{msa}$  for most cases likely to be encountered in practice

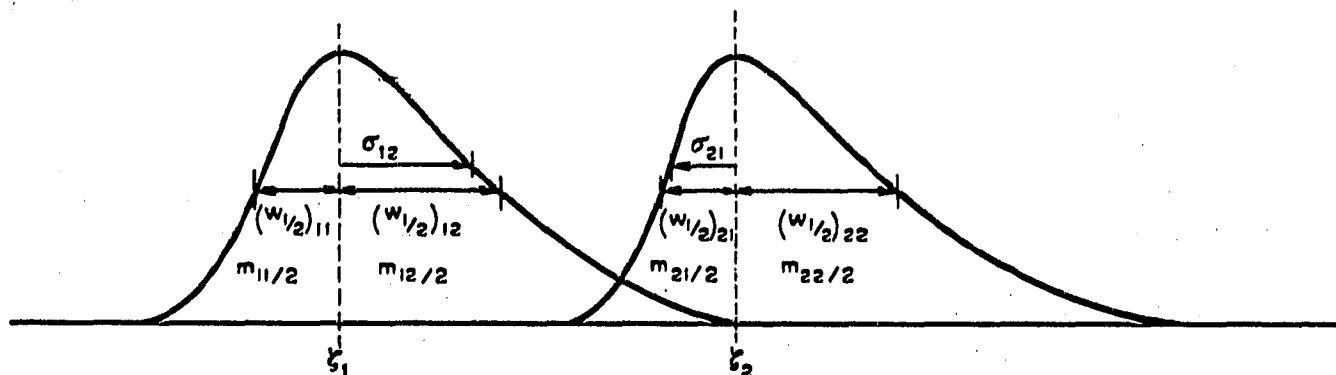


Fig. 1. Illustration of peak parameters.

\* Present address: Department of Chemistry, University of South Africa, Pretoria, South Africa.

(see APPENDIX I) and is particularly convenient since analytical expressions for the moments in non-linear chromatography are available<sup>3-5</sup>.

### THEORY

According to the references cited above the zero'th and first moments may be approximated by<sup>3</sup>

$$m_0 = m_1 \left\{ 1 + \frac{\lambda C_1}{2\sqrt{2}} \left[ 1 - \frac{1}{\left( 1 + \frac{4\pi D_e t}{w_1^2} \right)^{\frac{1}{2}}} \right] \right\} \quad (3)$$

and

$$\langle \zeta \rangle = Ut - \frac{\lambda C_1 U w_1^2}{4\sqrt{2}\pi D_e} \cdot \frac{m_1}{m_0} \left\{ \left[ 1 + \frac{4\pi D_e t}{w_1^2} \right]^{\frac{1}{2}} - 1 \right\} \quad (4)$$

where

$$U = u/(1 + k_1) \quad (5)$$

$$\lambda = 2k_2/(1 + k_1) \quad (6)$$

and  $k_1$  and  $k_2$  are defined by the non-linear isotherm

$$C_s = \varepsilon k_1 C + \varepsilon k_2 C^2 \quad (7)$$

$\lambda C_1$  is the non-linearity parameter,  $C_1$  is the initial solute concentration at the inlet in the mobile phase and  $m_1$  the number of moles.

The second moment will be approximated by<sup>4</sup>

$$\sigma_{nl}^2 = \sigma_l^2 \frac{m_1}{m_0} \left\{ 1 + \frac{\sigma_n^2}{\sigma_l^2} \right\} \quad (8)$$

where the linear contribution,  $\sigma_l^2$ , is given by

$$\sigma_l^2 = 2D_e t + \sigma_1^2 \quad (9)$$

and the non-linear contribution  $\sigma_n^2$  is, for convenience, written in the form

$$\sigma_n^2 = \sigma_n^2(D) + \sigma_n^2(u) \quad (10)$$

$\sigma_n^2(D)$  and  $\sigma_n^2(u)$  are contributions respectively associated with diffusion and flow and are given by

$$\begin{aligned} \sigma_n^2(D)/\sigma_l^2 = & \frac{\lambda C_1}{2\sqrt{2}} \cdot \frac{y}{1+y} - \frac{5\lambda C_1}{4\sqrt{2}} \cdot \left[ \frac{1}{(1+y)^{\frac{1}{2}}} - \frac{1}{(1+y)} \right] - \\ & - \frac{(\lambda C_1)^2}{8} \cdot \left[ \frac{1}{(1+y)^{\frac{1}{2}}} - \frac{1}{(1+y)} \right] + \frac{(\lambda C_1)^2}{16} \frac{\ln(1+y)}{1+y} \end{aligned} \quad (11)$$

and

$$\sigma_n^2(u)/\sigma_1^2 = \frac{\Omega}{8\pi} \cdot \frac{\lambda C_1 U w_1}{D_e} \cdot \frac{1}{2} \cdot \left[ \frac{2+y}{1+y} - \frac{2}{(1+y)^{\frac{1}{2}}} \right] \quad (12)$$

where

$$y = 4\pi D_e t / w_1^2$$

$\Omega$  is a semi-empirical fitting parameter ( $\Omega/8\pi \sim 10^{-2}$ ).

The above expressions for the moments were derived under the assumption of an equivalent Gaussian input<sup>6</sup> with the inlet variance given by

$$\sigma_1^2 = w_1^2 / 2\pi \quad (13)$$

$w_1$  is the width of the corresponding plug input.

In the analysis of refs. 3-5 the effective diffusion coefficient  $D_e$  was regarded as containing only terms deriving from the mobile phase. Since the nature of the stationary phase contributions is similar, however (e.g. ref. 7), it is expected that the approximation will also apply in this case and  $D_e$  will, in the present study, be regarded as containing contributions from both phases.

In order to simplify the above expressions for the statistical moments, the assumption of large  $y$  (either large  $t$  or small  $w_1$  or both) will now be made, *i.e.*

$$2D_e t \gg \sigma_1^2 = w_1^2 / 2\pi \quad (14)$$

so that

$$\sigma_1^2 \approx 2D_e t \quad (15)$$

To the first order in  $\lambda C_1$ , the expressions for  $m_0$  and  $\langle \zeta \rangle$  become

$$m_0 = m_1 \left\{ 1 + \frac{\lambda C_1}{2\sqrt{2}} \right\} \quad (16)$$

and

$$\langle \zeta \rangle = Ut - \frac{\lambda C_1 U w_1}{2\sqrt{2\pi D_e}} \cdot t^{\frac{1}{2}} \quad (17)$$

In the limit of large  $y$  the non-linear contributions to the variance are

$$\lim_{y \rightarrow \infty} \sigma_n^2(D)/\sigma_1^2 = \lambda C_1 / 2\sqrt{2} \quad (18)$$

and

$$\lim_{y \rightarrow \infty} \sigma_n^2(u)/\sigma_1^2 = \frac{\Omega}{8\pi} \cdot \frac{1}{2} \cdot \left[ \frac{\lambda C_1 U w_1}{D_e} \right]^2 \quad (19)$$

Since

$$U/D_e = 2/H_1 \quad (20)$$

where

$$H_1 = \sigma_1^2 / Ut, \quad (21)$$

Eqn. 19 becomes

$$\lim_{y \rightarrow \infty} \sigma_n^2(u)/\sigma_1^2 = 2 \frac{\Omega}{8\pi} \left[ \frac{\lambda C_1 w_1}{H_1} \right]^2 \quad (22)$$

For

$$H_1 \sim 0.14 w_1 \lambda C_1 \quad (23)$$

$\sigma^2(u)$  and  $\sigma_1^2$  become equal while for  $H_1$  smaller than this value, the velocity term is the dominant one.

It follows from eqns. 2 and 8 that, for  $m_1/m_0 \sim 1$  for both components,

$$R_{n1} = \frac{\langle \zeta \rangle_2 - \langle \zeta \rangle_1}{2\sigma_1} \left[ \left( 1 + \frac{(\sigma_n^2)_1}{\sigma_1^2} \right)^{\frac{1}{2}} + \left( 1 + \frac{(\sigma_n^2)_2}{\sigma_1^2} \right)^{\frac{1}{2}} \right]^{-1} \quad (24)$$

and for  $\sigma_2 = \sigma_1$ ,

$$R_{n1} = \frac{\langle \zeta \rangle_2 - \langle \zeta \rangle_1}{4\sigma_1} \left[ \left( 1 + \frac{(\sigma_n^2)_1}{\sigma_1^2} \right) \right]^{-\frac{1}{2}} \quad (25)$$

$R_{n1}$  will now be calculated for the instant when the mean of peak 1 reaches the detector, *i.e.* when

$$\langle \zeta \rangle_1 = l \quad (26)$$

The time corresponding to eqn. 26 is therefore the solution of the equation (see eqn. 17)

$$t - B(\lambda C_1)_1 t^{\frac{1}{2}} - l/U_1 = 0 \quad (27)$$

where the subscript 1 denotes component (peak) 1 and the notation  $k_{11}$  (for  $k_1$ ) and  $k_{21}$  (for  $k_2$ ) is used (see LIST OF SYMBOLS).  $B$  is given by

$$B = w_1 / (2\sqrt{2\pi D_e}) \quad (28)$$

(The subscript 1 is omitted for  $B$ , since it is assumed that  $D_e$  will be approximately the same for two solutes eluted close to each other.) The solution of eqn. 27 is

$$t^{\frac{1}{2}} = \frac{1}{2} B(\lambda C_1)_1 \left\{ 1 + \sqrt{1 + \frac{4l}{B^2(\lambda C_1)_1^2 U_1}} \right\} \quad (29)$$

*i.e.*

$$t = \frac{l}{U_1} + \frac{1}{2} B^2(\lambda C_1)_1^2 \left\{ 1 + \sqrt{1 + \frac{4l}{B^2(\lambda C_1)_1^2 U_1}} \right\} \quad (30)$$

$\langle \zeta \rangle_2$  corresponding to  $\langle \zeta \rangle_1 = l$  is obtained by using eqn. 30 for  $t$  in the expression for  $\langle \zeta \rangle_2$ , *i.e.*

$$\langle \zeta \rangle_2 = \frac{U_2}{U_1} l + \frac{1}{2} B^2(\lambda C_1)_1 U_2 \{ (\lambda C_1)_1 - (\lambda C_1)_2 \} \left\{ 1 + \sqrt{1 + \frac{4l}{B^2(\lambda C_1)_1^2 U_1}} \right\} \quad (31)$$

so that the distance between the means of the peaks is:

$$\langle \zeta \rangle_2 - \langle \zeta \rangle_1 = l \left( \frac{U_2}{U_1} - 1 \right) + \frac{1}{2} B^2(\lambda C_1)_1^2 (1 - \beta) \left\{ 1 + \sqrt{1 + \frac{4l}{B^2(\lambda C_1)_1^2 U_1}} \right\}$$

*i.e.*

$$\langle \zeta \rangle_2 - \langle \zeta \rangle_1 = \frac{l k_{12}(\alpha - 1)}{1 + k_{12}} + \frac{1}{2} B^2 (\lambda C_1)_1^2 U_2 (1 - \beta) \left\{ 1 + \sqrt{1 + \frac{4l}{B^2 (\lambda C_1)_1^2 U_1}} \right\} \quad (32)$$

where

$$\alpha = k_{11}/k_{12} \quad (33)$$

and

$$\beta = (\lambda C_1)_2 / (\lambda C_1)_1 \quad (34)$$

If  $H_1$  is defined as the plate height for component 1, eluted according to a linear isotherm, then (see eqn. 21)

$$\sigma_1^2 = H_1 U_1 t \quad (35)$$

and (from eqns. 15 and 35)

$$D_e = \frac{H_1}{2} U_1 \quad (36)$$

$U_1 t$  will now, according to eqn. 30, be approximated by  $l$  so that

$$\sigma_1^2 = H_1 l \quad (37)$$

From eqns. 28, 32, 36 and 37 it then follows that

$$\frac{\langle \zeta \rangle_2 - \langle \zeta \rangle_1}{\sigma_1} = \sqrt{\frac{l}{H_1}} \frac{k_{12}(\alpha - 1)}{(1 + k_{12})} + \frac{w_1^2}{8\pi} \frac{1}{H_1^{\frac{1}{2}} l^{\frac{1}{2}}} \left( \frac{1 + k_{11}}{1 + k_{12}} \right) (\lambda C_1)_1^2 (1 - \beta) \left[ 1 + \left( 1 + \frac{16\pi}{w_1^2} l H_1 \frac{1}{(\lambda C_1)_1^2} \right)^{\frac{1}{2}} \right] \quad (38)$$

An approximate expression for  $R_{n1}$  may therefore be obtained by using eqn. 38 together with the appropriate expressions for the non-linear  $\sigma^2$  contributions in either eqn. 24 or 25. At large values of  $y$ ,  $R_{n1}$  is approximated by (eqns. 18, 22 and 24)

$$R_{n1} = \frac{\langle \zeta \rangle_2 - \langle \zeta \rangle_1}{2\sigma_1} \left\{ \left[ 1 + \frac{(\lambda C_1)_1^2}{2\sqrt{2}} + 2 \frac{\Omega}{8\pi} \left( \frac{(\lambda C_1)_1 w_1}{H_1} \right)^2 \right]^{\frac{1}{2}} + \left[ 1 + \frac{(\lambda C_1)_2^2}{2\sqrt{2}} + 2 \frac{\Omega}{8\pi} \left( \frac{(\lambda C_1)_2 w_1}{H_1} \right)^2 \right]^{\frac{1}{2}} \right\}^{-1} \quad (39)$$

for  $\sigma_2 \neq \sigma_1$ , or by eqns. 18, 22 and 25

$$R_{n1} = \frac{\langle \zeta \rangle_2 - \langle \zeta \rangle_1}{4\sigma_1} \left\{ 1 + \frac{(\lambda C_1)_1^2}{2\sqrt{2}} + 2 \frac{\Omega}{8\pi} \left( \frac{(\lambda C_1)_1 w_1}{H_1} \right)^2 \right\}^{-\frac{1}{2}} \quad (40)$$

for  $\sigma_2 = \sigma_1$ , with  $(\langle \zeta \rangle_2 - \langle \zeta \rangle_1)/\sigma_1$  given by eqn. 38.

An improved approximation for  $R_{n1}$  may be obtained by approximating  $l$ , *i.e.*  $\langle \zeta \rangle_1$  (see eqn. 4), by

$$l = U_1 t - \frac{(\lambda C_1)_1 U_1 w_1}{2\sqrt{2\pi D_e}} t^{\frac{1}{2}} + \frac{(\lambda C_1)_1 U_1 w_1^2}{4\sqrt{2\pi D_e}} \quad (41)$$

from which  $t$  follows as

$$t = \frac{l}{U_1} - \sqrt{2} B^2 (\lambda C_1)_1 + \frac{1}{2} A^2 (\lambda C_1)_1^2 \left\{ 1 + \sqrt{1 + \frac{4l}{B^2 (\lambda C_1)_1^2 U_1} - \frac{4\sqrt{2}}{(\lambda C_1)_1}} \right\} \quad (42)$$

The separation of the means of the two peaks is now given by

$$\begin{aligned} \frac{\langle \zeta \rangle_2 - \langle \zeta \rangle_1}{\sigma_1} &= \sqrt{\frac{l}{H_1}} \frac{k_{12}(\alpha - 1)}{(1 + k_{12})} + \frac{w_1^2}{8\pi} \frac{1}{H_1^{\frac{3}{2}} l^{\frac{1}{2}}} \left( \frac{1 + k_{11}}{1 + k_{12}} \right) (\lambda C_1)_1^2 (1 - \beta) \times \\ &\times \left[ 1 + \left( 1 + \frac{16\pi}{w_1^2} l H_1 \frac{1}{(\lambda C_1)_1^2} - \frac{4\sqrt{2}}{(\lambda C_1)_1} \right)^{\frac{1}{2}} \right] - \frac{\sqrt{2} w_1^2}{4\pi} \frac{1}{H_1^{\frac{3}{2}} l^{\frac{1}{2}}} \left( \frac{1 + k_{11}}{1 + k_{12}} \right) (\lambda C_1)_1 (1 - \beta) \end{aligned} \quad (43)$$

which may be used in the above expressions for  $R_{nl}$ .

#### EVALUATION OF THEORETICAL RESULTS

The validity of the approximations involved in the derivation of the expressions for  $R_{nl}$  and the relationship between  $R_{nl}$  and  $R_{msa}$  were evaluated by means of computer simulation (e.g. ref. 3) of non-linear elution chromatography. The simulation program provided values for  $R_{nl}$  according to eqn. 2. These were then compared with the theoretically predicted values from eqn. 24. The comparison between  $R_{msa}$  and  $R_{nl}$  was effected by measuring the parameters required for the calculation for  $R_{msa}$  in eqn. 1 from the plotted simulation peaks (see Fig. 1); the compo-

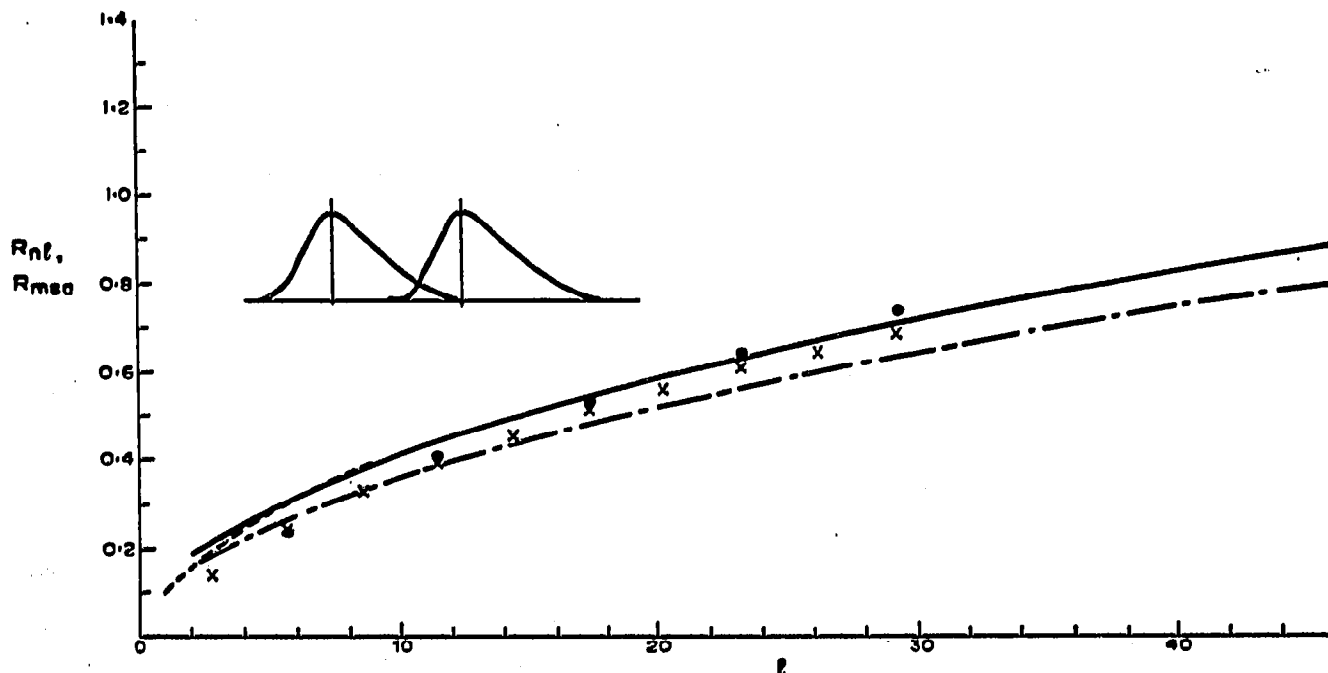


Fig. 2. Resolution as a function of column length.  $(\lambda C_1)_1 = 0.5$ ,  $(\lambda C_1)_2 = 0.5$ ,  $k_{11} = 30$ ,  $k_{12} = 20$ ,  $D_e = 0.01$ ,  $w_1 = 4.8$  cm,  $u = 1$  cm/sec. Simulation results:  $\times$ ,  $R_{nl}$ ;  $\bullet$ ,  $R_{msa}$ .

peaks for such pairs were obtained by superposition of individually simulated peaks).  $\sigma_{12}$  and  $\sigma_{21}$  are obtained from  $(w_{1/2})_{12}$  and  $(w_{1/2})_{21}$  in terms of the bi-Gaussian<sup>1</sup> approximation, e.g.,

$$\sigma_{12} = (w_{1/2})_{12} / 1.177 \quad (44)$$

The calculations were carried out for  $\alpha = 1.5$  and various combinations of  $D_e$ ,  $(\lambda C_1)_1$  and  $(\lambda C_1)_2$ . These results are graphically represented in Figs. 2-6. Each

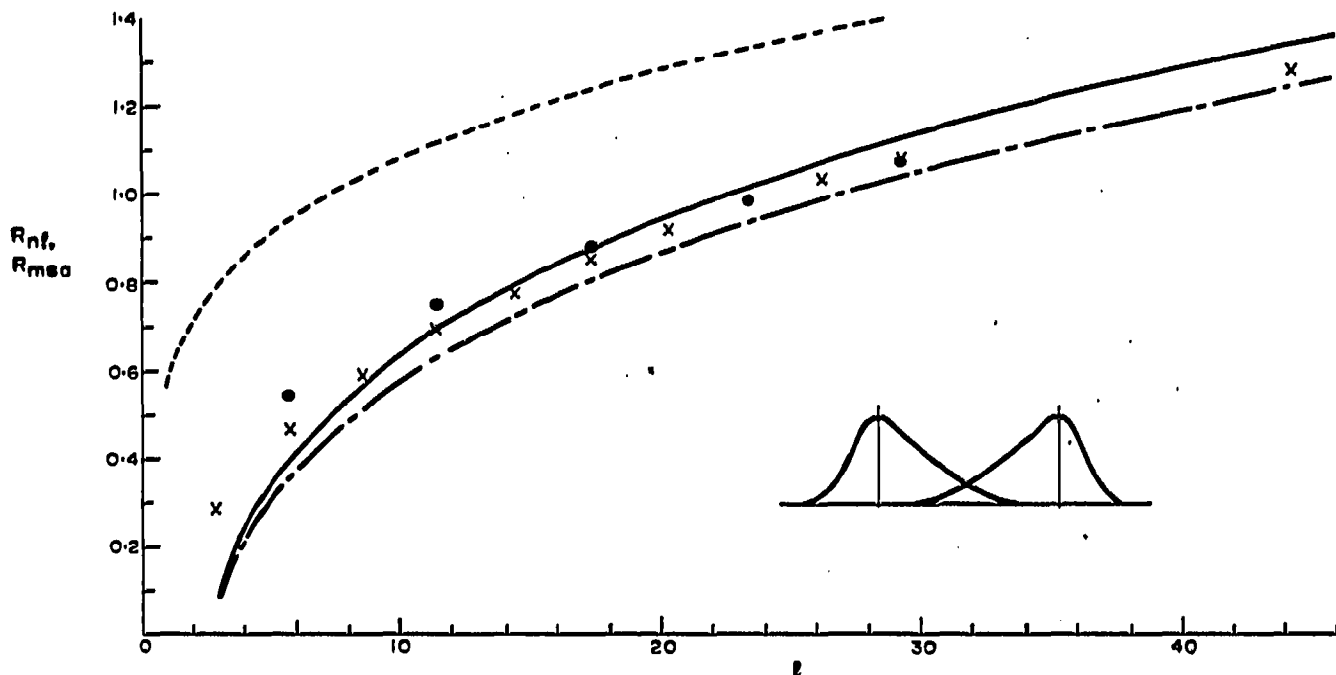


Fig. 3. Resolution as a function of column length.  $(\lambda C_1)_1 = 0.5$ ,  $(\lambda C_1)_2 = -0.5$ ,  $k_{11} = 30$ ,  $k_{12} = 20$ ,  $D_e = 0.01$ ,  $w_1 = 4.8$  cm,  $u = 1$  cm/sec. Simulation results:  $\times$ ,  $R_{nl}$ ;  $\bullet$ ,  $R_{msa}$ .

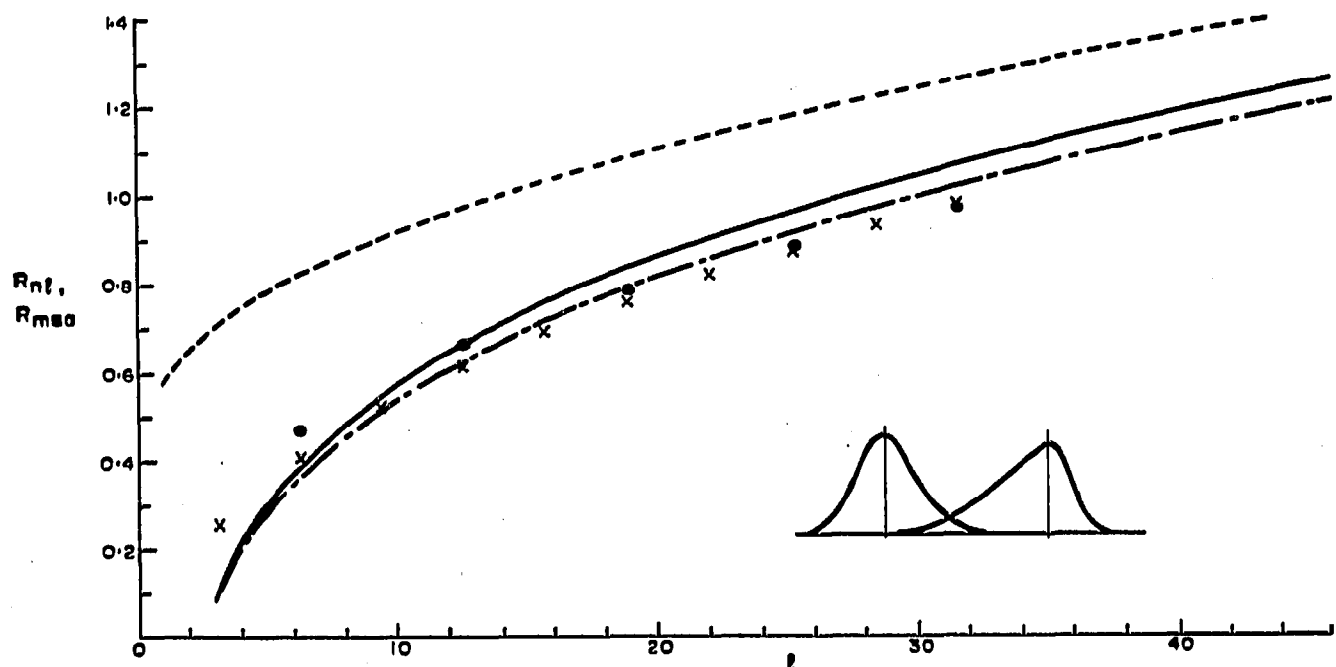


Fig. 4. Resolution as a function of column length.  $(\lambda C_1)_1 = 0.1$ ,  $(\lambda C_1)_2 = -0.5$ ,  $k_{11} = 30$ ,  $k_{12} = 20$ ,  $D_e = 0.01$ ,  $w_1 = 4.8$  cm,  $u = 1$  cm/sec. Simulation results:  $\times$ ,  $R_{nl}$ ;  $\bullet$ ,  $R_{msa}$ .

figure is accompanied by a schematic representation of the peak pair which it describes. In all cases  $R_{msa}$  and various approximations of  $R_{nl}$  are represented as functions of column length,  $l$ . Three approximations of  $R_{nl}$  are given: (i) eqns. 24 and 38 (----); (ii) eqn. 24 and the improved  $(\langle \zeta \rangle_2 - \langle \zeta \rangle_1) / \sigma_1$  value from eqn. 43 (—); and (iii) eqns. 39 and 43 (— · — · —).

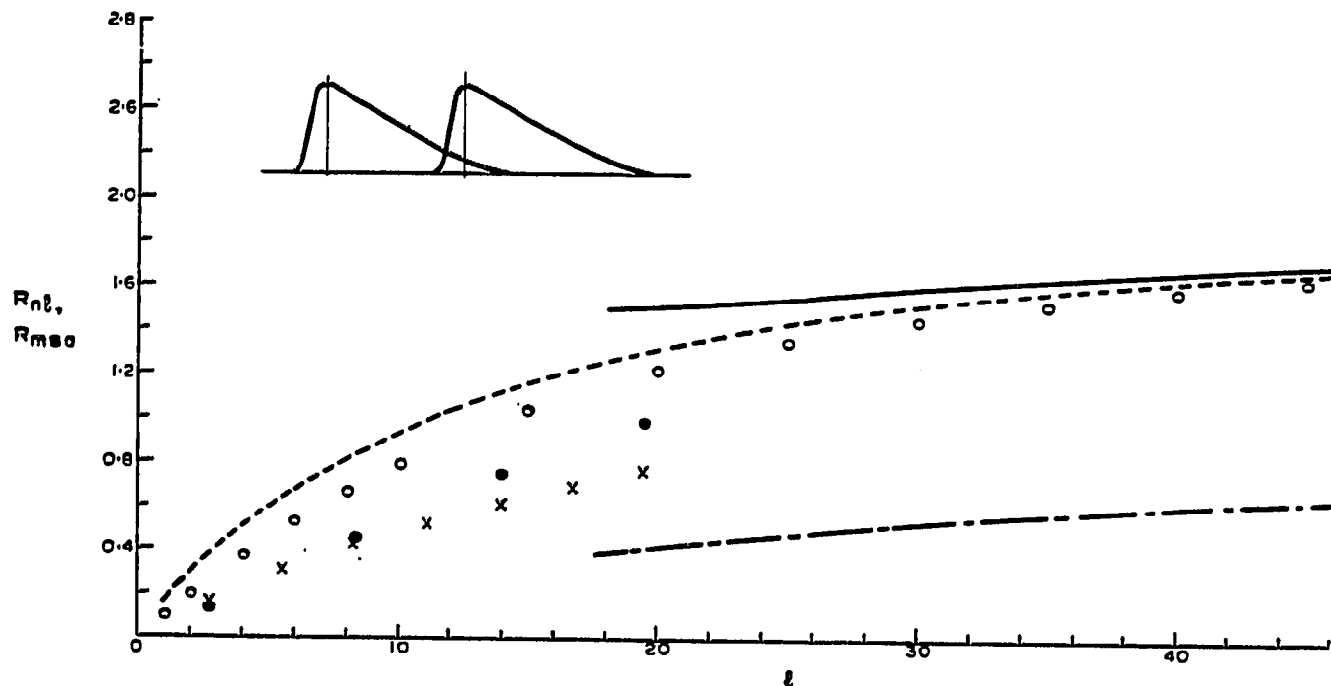


Fig. 5. Resolution as a function of column length.  $(\lambda C_1)_1 = 0.5$ ,  $(\lambda C_1)_2 = 0.5$ ,  $k_{11} = 30$ ,  $k_{12} = 20$ ,  $D_e = 0.001$ ,  $w_1 = 4.8$  cm,  $u = 1$  cm/sec. Simulation results:  $\times$ ,  $R_{nl}$ ;  $\bullet$ ,  $R_{msa}$ .

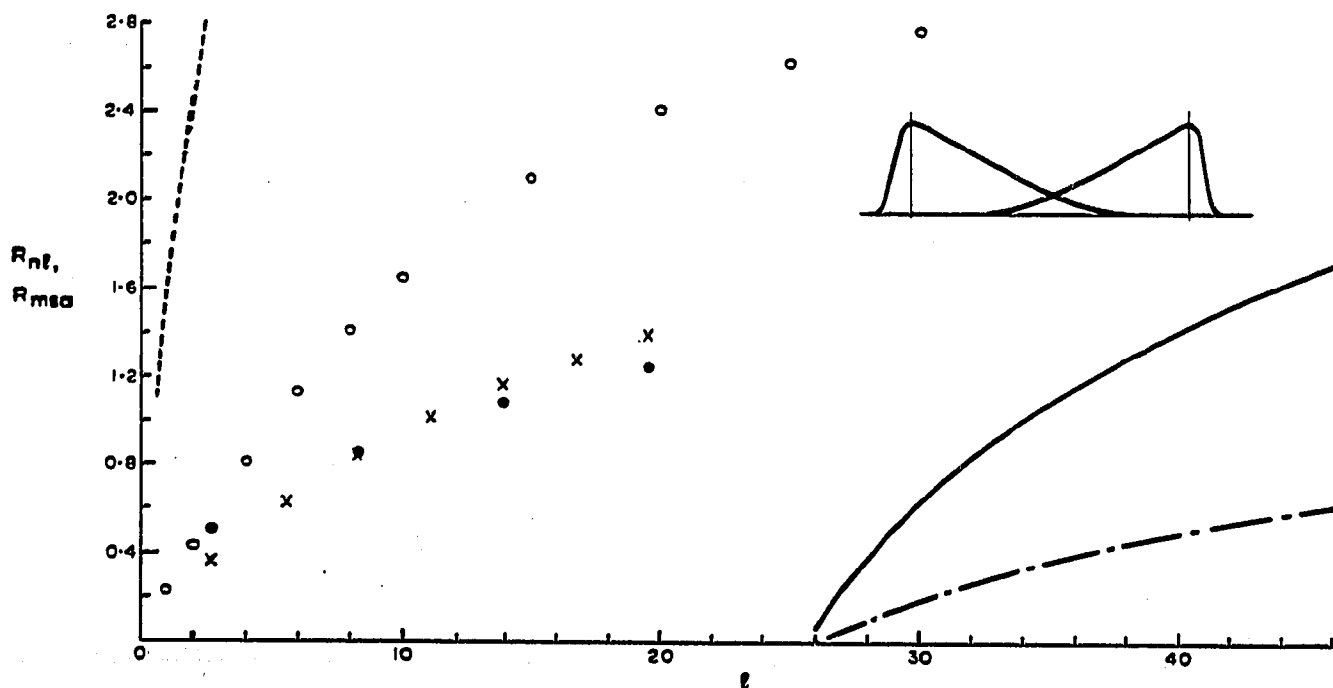


Fig. 6. Resolution as a function of column length.  $(\lambda C_1)_1 = 0.5$ ,  $(\lambda C_1)_2 = -0.5$ ,  $k_{11} = 30$ ,  $k_{12} = 20$ ,  $D_e = 0.001$ ,  $w_1 = 4.8$  cm,  $u = 1$  cm/sec. Simulation results:  $\times$ ,  $R_{nl}$ ;  $\bullet$ ,  $R_{msa}$ .



TABLE I

THEORETICAL RELATIONSHIP BETWEEN  $R_{nl}$  AND  $R_{msa}$ 

Peak pair <sup>a</sup>		$R_{msa}$ range (simulation)	$A$ (simulation)	$R_{nl}/R_{msa}$ (simulation)	$R_{nl}/R_{msa}$ (eqn. I-7)
Peak 1	Peak 2				
$C_1 = 0.1^b$	$C_1 = 0.5$	0.12-0.55	0.1338	1.57-1.0355	1.6687-1.0536
$C_1 = 0.5^b$	$C_1 = 0.5$	0.236-0.7375	0.0476	1.045-0.9338	1.1086-1.0038
$C_1 = 0.1^b$	$C_1 = -0.5$	0.4711-0.9749	-0.1642	0.8678-1.0	0.8629-1.0353
$C_1 = 0.5^b$	$C_1 = -0.5$	0.5474-1.0789	-0.2107	0.8460-1.0	0.8769-1.0
$C_1 = 0.5^c$	$C_1 = 0.5$	0.1368-0.98	0.0888	1.2113-0.7823	1.3958-0.9850
$C_1 = 0.5^c$	$C_1 = -0.5$	0.5086-1.2458	-0.4105	0.7277-1.1251	0.6010-1.2492

<sup>a</sup>  $k_{11} = 30$ ,  $k_{12} = 20$ ,  $\alpha = 1.5$ ,  $w_1 = 4.8$  cm,  $u = 1$  cm/sec.<sup>b</sup>  $D_e = 0.01$ .<sup>c</sup>  $D_e = 0.001$ .

The theoretical relationship between  $R_{nl}$  and  $R_{msa}$  as derived in APPENDIX I was also investigated by comparing  $R_{nl}/R_{msa}$  values obtained from the simulation results with those calculated from eqn. I-7. The required  $A$  values were obtained by actual measurement of the simulated peaks as were the  $R_{msa}$  values which are common to both cases. Table I summarizes these results. For each peak pair considered the variation of  $A$  with  $l$  was slight and an average  $A = \langle A \rangle$  was used in the calculations.

## DISCUSSION

Figs. 2-6 allow several conclusions regarding the approximations to be made. Deviations are apparently associated with small  $y$  values (*i.e.* when  $l$  and/or  $D_e/w_1^2$  are small). Small  $y$  values can affect the predictions in a variety of ways, *e.g.*: (i) Breakdown of the mathematical approximation  $y \gg 1$  in eqns. 38 and 43. (ii) The expressions for the moments themselves involve approximations in the evaluation of integrals in which the actual peak is replaced by one of Gaussian form (*e.g.* ref. 3). In cases where extreme deviations from the Gaussian occur, deviations can therefore be expected. This is particularly true for systems with small  $D_e$  values in which a triangular distribution is approached. (iii) Higher order terms become increasingly important as  $y$  decreases with constant  $\lambda C_1$ . An indication of the relative importance of the above mechanisms is provided in Figs. 5 and 6, where the removal of restriction (i) is seen not to improve the results to the extent one would intuitively expect. (In Figs. 5 and 6 the circled values (⊙) were obtained by solving for  $l$  directly from eqn. 4 without simplifying assumptions.) Effects (ii) and (iii) can therefore have a pronounced effect. The situation represented by Fig. 5 or 6 is, however, an extreme case and for the cases represented in Figs. 2-4 the correspondence of the actual  $R_{nl}$  values and those predicted by the improved equation (eqn. 43) is generally good except for the expected deterioration with small  $D_e/w_1^2$  values. Predictions based on eqn. 38 invariably show more marked deviations and although it may therefore be useful due to its simplicity, it should only be used for qualitative description.

The results tabulated in Table I give support to the theoretically derived relationship between  $R_{nl}$  and  $R_{msa}$ . Eqn. (I-7) can therefore be used as a means of

relating the impurity ratio via  $R_{msa}$  and  $R_{nl}$  to the column parameters. In situations where  $A$  (eqn. I-8) is not known beforehand,  $R_{nl}$  and  $R_{msa}$  may be equated to a first approximation. An idea of the errors involved in this approximation may be inferred from Fig. 7, where the ratio  $R_{nl}/R_{msa}$  has been plotted as a function of  $A$  for a representative range of  $R_{msa}$  values.

An important practical consequence of the present analysis is the possibility of predicting the column length required for a specified impurity ratio. This would involve firstly the determination of the required  $R_{msa}$  value which is consequently related to the  $R_{nl}$  value by means of eqn. I-7. The column length can then be read off from, e.g. Fig. 2. Consider the peaks with parameter values given in Table II. These peaks could, for instance, comprise a chromatogram region in which an improved resolution is desired. Alternatively, known components of a mixture may be injected separately to obtain these parameter values. In principle the  $s$  and  $m$  values (see Fig. 1)

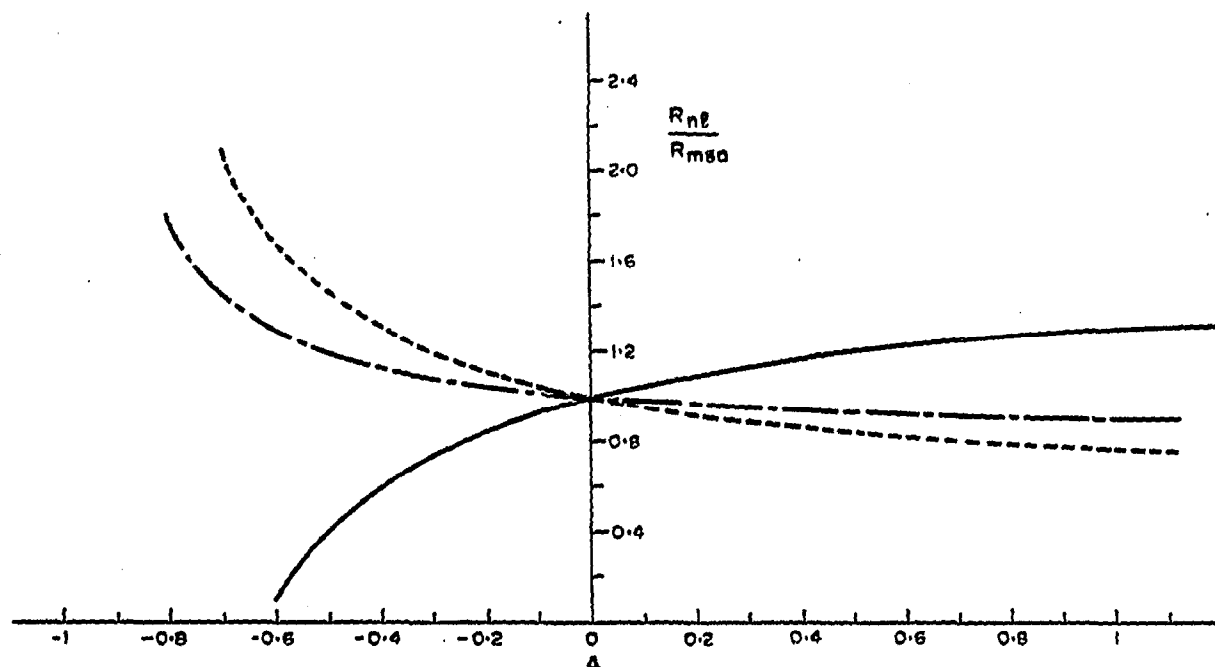


Fig. 7. Theoretical relationship between  $R_{nl}$  and  $A$  (eqn. I-7). —,  $R_{msa} = 0.5$ ; - - - - -,  $R_{msa} = 1.0$ ; - · - · -,  $R_{msa} = 1.5$ .

TABLE II

PEAK PAIR CONSIDERED IN EXAMPLE

Peak 1		Peak 2		
$k_{11}$	30	$k_{12}$	20	$\alpha = 1.5$
$(\lambda C_1)_1$	0.5	$(\lambda C_1)_2$	0.5	$\beta = 1$
$D_e$	0.01	$D_e$	0.01	
$w_1$	4.8	$w_1$	4.8	
$(w_{1/2})_{11}$	4.32	$(w_{1/2})_{21}$	3.87	
$(w_{1/2})_{12}$	6.6	$(w_{1/2})_{22}$	7.23	
$\zeta_1$	27.378	$\zeta_2$	40.499	
$m_{01}$	2.623	$m_{02}$	2.629	

$$s_p = \sigma_{21}/\sigma_{12} = (w_{\frac{1}{2}})_{21}/(w_{\frac{1}{2}})_{12} \quad (45)$$

$$s_{2a} = \sigma_{22}/\sigma_{21} = (w_{\frac{1}{2}})_{22}/(w_{\frac{1}{2}})_{21} \quad (46)$$

and

$$m_p = m_{21}/m_{12} \quad (47)$$

required to relate  $R_{msa}$  to the impurity ratio  $\eta$  (ref. 2) can be theoretically predicted although this is not a practical procedure. A similar situation exists in linear chromatography for the overall peak width ratio,  $s$ . Once these values are known, specification of the impurity ratio,  $\eta$ , uniquely defines  $R_{msa}$  in terms of  $\eta$  (see Fig. 8).

For the above example ( $l = 29.2$ )

$$R_{msa} = 0.7375$$

$$s_p = 0.5864$$

and

$$m_p = 0.5781$$

so that it follows from Fig. 8 that

$$\eta = 0.075$$

The success of the theoretical model in predicting column lengths required

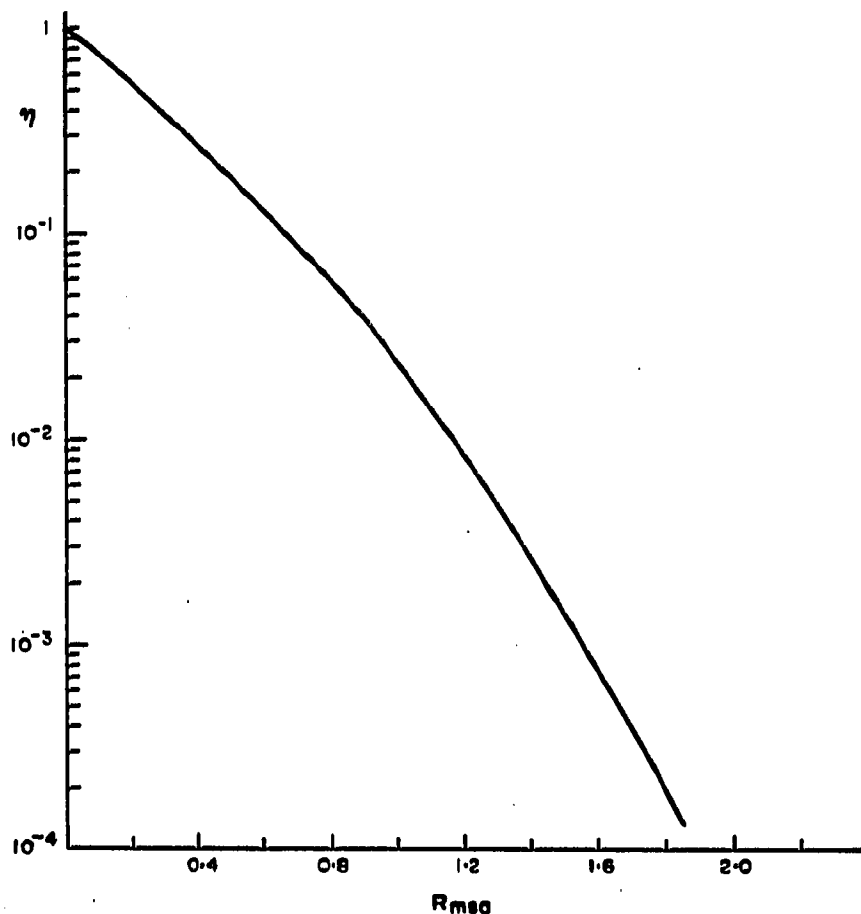


Fig. 8. Impurity ratio as a function of  $R_{msa}$  (for peak pair in Table II).

for different purity specifications ( $\eta$ ) can now be gauged by calculating these lengths and comparing them to the actual lengths at which these purities were actually reached. For all the cases, the  $A$  value (0.0516) corresponding to  $l = 29.2$  was used and the same  $R_{msa}-\eta$  relationship (Fig. 8) was used throughout. The results are tabulated in Table III. The correspondence is satisfactory in the light of the approximations involved.

TABLE III  
COLUMN LENGTHS REQUIRED FOR SPECIFIED PURITIES

$\eta$	$R_{msa}$ (Fig. 8)	$R_n$ (eqn. I-7)	$l$ (cm) (Fig. 2)	$l$ (cm) (actual)
0.46	0.24	0.238	4.2	5.7
0.26	0.4	0.396	9.8	11.5
0.16	0.54	0.535	17	17.3
0.11	0.54	0.634	23.6	23.3
0.075	0.64	0.733	31.2	29.2

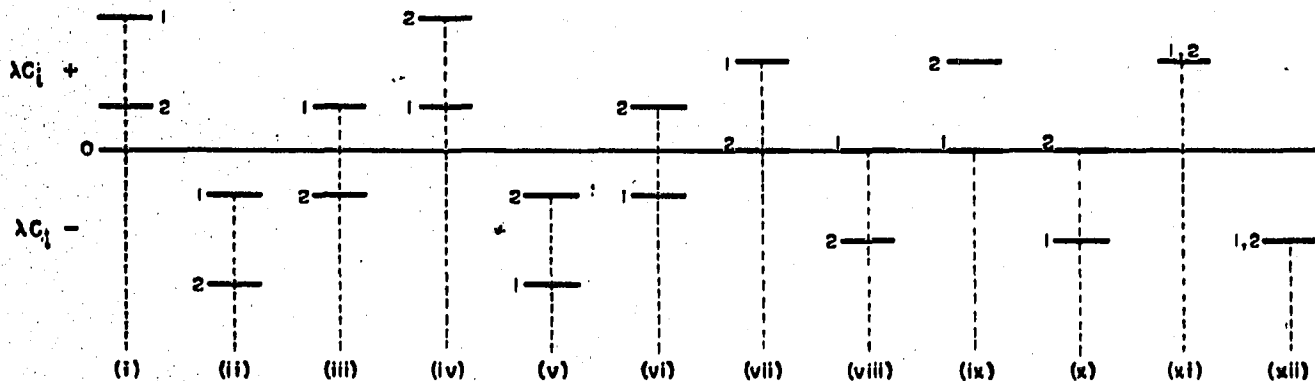


Fig. 9. Schematic representation of possible peak pair combinations.

In non-linear chromatography there are actually twelve possible combinations of  $(\lambda C_1)_1$  and  $(\lambda C_1)_2$ , each leading to a characteristic non-linear peak pattern. These are schematically represented in Fig. 9. A systematic qualitative analysis of the behaviour of  $R_{n1}$  relative to  $R_n$  for the cited cases is made possible by an analysis of the approximate equation

$$R_{n1} = \frac{\langle \zeta \rangle_2 - \langle \zeta \rangle_1}{4\sigma_1} \quad (48)$$

with  $(\langle \zeta \rangle_2 - \langle \zeta \rangle_1)/\sigma_1$  given by eqn. 38. Effects relating to non-linear second moment contributions to  $R_{n1}$  is thus neglected in the present approximation. In addition it will be assumed that

$$\left\{ 1 + \frac{16\pi}{w_1^2} |H_1| \frac{1}{(\lambda C_1)_1^2} \right\}^{\frac{1}{2}} \approx \frac{4\sqrt{\pi}}{w_1^2} \sqrt{|H_1|} \frac{1}{(\lambda C_1)_1} \quad (49)$$

so that

$$R_{n1} - R_n = \Delta_1 \left\{ 1 + \frac{\Delta_2}{\Delta_1} \right\} \quad (50)$$

where

$$R_n = \frac{1}{4} \sqrt{\frac{l}{H_1}} \frac{k_{12}(\alpha - 1)}{(1 + k_{12})} \tag{51}$$

and  $\Delta_1$  and  $\Delta_2$  are given by

$$\Delta_1 = \frac{w_1^2}{32\pi} \cdot \frac{1}{H_1^{\frac{3}{2}} l^{\frac{1}{2}}} \left( \frac{1 + k_{11}}{1 + k_{12}} \right) (\lambda C_1)_1 [(\lambda C_1)_1 - (\lambda C_1)_2] \tag{52}$$

and

$$\Delta_2 = \frac{w_1}{8\sqrt{\pi}} \cdot \frac{1}{H_1} \left( \frac{1 + k_{11}}{1 + k_{12}} \right) [(\lambda C_1)_1 - (\lambda C_1)_2] \tag{53}$$

Application of these results to the cases depicted in Fig. 9 are summarized in Table IV. Actual inspection of the numerical computations showed that for case (v),  $|\Delta_2/\Delta_1| < 1$ . It should be noted that  $R_n$  is only equal to the linear resolution,  $R_1$ , when  $U_1 t = l$  since

$$R_1 = \frac{1}{4} \sqrt{\frac{U_1 t}{H_1}} \frac{k_{12}(\alpha - 1)}{(1 + k_{12})} \tag{54}$$

and interpretation of the above scheme in terms of  $R_1$  thus requires a knowledge of the ratio  $U_1 t/l$ .

Although these phenomena were not considered in detail in the present paper, it is interesting to note that for small  $\alpha$  values ( $\sim 1.1$ ) certain specific  $(\lambda C_1)_1$  and  $(\lambda C_1)_2$  combinations (e.g.  $(\lambda C_1)_1 = -0.5$ ,  $(\lambda C_1)_2 = 0.5$ ) lead to peak pairs in which the elution sequence (as determined by the  $\langle \zeta \rangle$  values) is inverted relative to that for the linear ( $\lambda = 0$ ) case. This results when non-linearity is so pronounced that it dominates the linear peak separating ability characterized mainly by  $\alpha$ .

TABLE IV  
CLASSIFICATION SCHEME FOR NON-LINEAR PEAK PATTERNS

Case	$\Delta_1$	$\Delta_2$	$\frac{\Delta_2}{\Delta_1}$	$\left  \frac{\Delta_2}{\Delta_1} \right $	$R_{nl} - R_n$
(i)	$> 0$	$< 0$	+	$\begin{matrix} < 1 \\ > 1 \end{matrix}$	$\begin{matrix} > 0 \\ > 0 \end{matrix}$
(ii)	$< 0$	$> 0$	-	$\begin{matrix} < 1 \\ > 1 \end{matrix}$	$\begin{matrix} < 0 \\ < 0 \end{matrix}$
(iii)	do (i)				
(iv)	$< 0$	$< 0$	+	$\begin{matrix} < 1 \\ > 1 \end{matrix}$	$\begin{matrix} < 0 \\ < 0 \end{matrix}$
(v)	$> 0$	$< 0$	-	$\begin{matrix} < 1 \\ > 1 \end{matrix}$	$\begin{matrix} > 0 \\ < 0 \end{matrix}$
(vi)	do (v)				
(vii)	do (i)				
(viii)	0	$> 0$	-	-	$> 0$
(ix)	0	$< 0$	-	-	$< 0$
(x)	do (v)				
(xi)	0	0	-	-	$= 0$
(xii)	do (xi)				

## APPENDIX I

*Relationship between  $R_n$  and  $R_{msa}$* 

$R_{n1}$  and  $R_{msa}$  are given by

$$R_{n1} = \frac{\langle \zeta \rangle_2 - \langle \zeta \rangle_1}{2(\sigma_1 + \sigma_2)} \quad (\text{I-1})$$

and

$$R_{msa} = \frac{\zeta_2 - \zeta_1}{2(\sigma_{12} + \sigma_{21})} \quad (\text{I-2})$$

If the peaks are fitted by means of bi-Gaussian distribution functions, the means and standard deviations appearing in eqn. I-1 may be approximated by<sup>1</sup> (see Fig. 1)

$$\langle \zeta \rangle_1 = \zeta_1 + \sqrt{\frac{2}{\pi}} (\sigma_{12} - \sigma_{11}) \quad (\text{I-3})$$

$$\langle \zeta \rangle_2 = \zeta_2 + \sqrt{\frac{2}{\pi}} (\sigma_{22} - \sigma_{21}) \quad (\text{I-4})$$

$$\sigma_1 = \frac{1}{2}(\sigma_{11} + \sigma_{12}) \quad (\text{I-5})$$

and

$$\sigma_2 = \frac{1}{2}(\sigma_{21} + \sigma_{22}) \quad (\text{I-6})$$

Substitution into eqn. I-1 gives, upon rearrangement,

$$R_{n1} = R_{msa} \left( \frac{1 + \sqrt{\frac{2}{\pi}} A}{1 + A} \right) \quad (\text{I-7})$$

where

$$\begin{aligned} A &= \frac{\sigma_{22} + \sigma_{11}}{2(\sigma_{12} + \sigma_{21})} - \frac{1}{2} = \\ &= \frac{(w_{\frac{1}{2}})_{22} + (w_{\frac{1}{2}})_{11}}{2[(w_{\frac{1}{2}})_{12} + (w_{\frac{1}{2}})_{21}]} - \frac{1}{2} \end{aligned} \quad (\text{I-8})$$

It follows from eqn. I-7 that for small values of  $|A|$  and for  $R_{msa} = \sqrt{2/\pi} \approx 0.8$ ,  $R_{n1} \approx R_{msa}$ . Eqn. I-7 is represented graphically in Fig. 7, where  $R_{n1}/R_{msa}$  is plotted as a function of  $A$  for various values of  $R_{msa}$ .

## LIST OF SYMBOLS

- $A$  convenient parameter, eqn. I-8
- $B$  convenient parameter, eqn. 28
- $C$  solute concentration in mobile phase
- $C_1$  value of  $C$  at the inlet at time  $t = 0$
- $C_s$  concentration of adsorbed solute
- $D_e$  effective diffusion coefficient due to mobile phase non-equilibrium
- $H_i$  plate height for linear ( $\lambda = 0$ ) elution chromatography (eqn. 21)
- $h_i$  ( $i = 1, 2$ ) parameters in non-linear distribution isotherm (eqn. 7)

$k_{ij}$	( $i = 1,2; j = 1,2$ ), $k_i$ for component (peak) $j$
$l$	column length
$m_1$	mass of solute per unit cross-section of the mobile phase at the inlet at time $t = 0$
$m_0$	zero'th moment
$m_{0j}$	( $j = 1,2$ ), $m_0$ for component $j$
$m_{ij}$	( $j = 1,2; j = 1,2$ ) mass parameters for asymmetrical (bi-Gaussian) peaks (see Fig. 1)
$m_p$	$= m_{21}/m_{12}$ , convenient parameter
$R_1$	resolution in linear chromatography (eqn. 54)
$R_{msa}$	resolution function related to purity specification
$R_n$	contribution to $R_{n1}$ (eqn. 51)
$R_{n1}$	resolution function related to column parameters
$s_2a$	$= \sigma_{22}/\sigma_{21}$ , skewness parameter of (bi-Gaussian) peak 2
$s_p$	$= \sigma_{21}/\sigma_{12}$ , convenient parameter
$t$	time
$u$	carrier flow velocity
$U$	$= u/(1 + k_1)$
$U_j$	$= u/(1 + k_{1j})$ ( $j = 1,2$ ), $u$ for component $j$
$w_1$	width of plug inlet sample profile
$(w^{1/2})_{ij}$	( $i = 1,2; j = 1,2$ ) width-at-halfheight parameters (see Fig. 1)
$y$	$= 4\pi D_e t/w_1^2$ , dimensionless time parameter
$\zeta_j$	( $j = 1,2$ ) position of maximum of $j$ 'th peak (Fig. 1)
$\langle \zeta \rangle_j$	( $j = 1,2$ ) position of mean of $j$ 'th peak

## GREEK SYMBOLS

$\alpha$	$= k_{11}/k_{12}$
$\beta$	$= (\lambda C_1)_2/(\lambda C_1)_1$
$\Delta_1$	convenient parameter (eqn. 52)
$\Delta_2$	convenient parameter (eqn. 53)
$\varepsilon$	void fraction
$\eta$	impurity ratio
$\lambda$	$= 2k_2/(1 + k_1)$ , non-linearity parameter
$\sigma_j$	( $j = 1,2$ ) standard deviation of peak $j$
$\sigma_{ij}$	$= w_{ij}/1.77$ ( $i = 1,2; j = 1,2$ ), (bi-Gaussian) peak standard deviation parameters (see Fig. 1)
$\sigma_1$	standard deviation of peak eluted under linear conditions ( $\lambda = 0$ )
$\sigma_1^2$	inlet variance
$\sigma_1^2$	variance of peak eluted under linear conditions (linear contribution to $\sigma_{n1}^2$ )
$\sigma_n^2$	non-linear contribution to $\sigma_{n1}^2$
$(\sigma_n^2)_j$	( $j = 1,2$ ), $\sigma_n^2$ for peak $j$
$\sigma_{n1}^2$	total variance in non-linear chromatography
$\sigma_n^2(D)$	diffusional contribution to $\sigma_n^2$
$\sigma_n^2(u)$	flow contribution to $\sigma_n^2$
$\Omega$	convenient semi-empirical fitting parameter (see eqn. 12)

## REFERENCES

- 1 T. S. BUYS AND K. DE CLERK, *Anal. Chem.* in press.
- 2 T. S. BUYS AND K. DE CLERK, *Sep. Sci.*, submitted for publication.
- 3 K. DE CLERK AND T. S. BUYS, *J. Chromatogr.*, 63 (1971) 193.
- 4 T. S. BUYS AND K. DE CLERK, *J. Chromatogr.*, 67 (1972) 1.
- 5 T. S. BUYS AND K. DE CLERK, *J. Chromatogr.*, 67 (1972) 13.
- 6 K. DE CLERK, T. S. BUYS AND V. PRETORIUS, *Sep. Sci.*, 6 (1971) 733.
- 7 T. S. BUYS AND K. DE CLERK, *Sep. Sci.*, submitted for publication.

*J. Chromatogr.*, 69 (1972) 87-102